

## Nanoscrews: Asymmetrical Etching of Silver Nanowires

Rachel Lee Siew Tan,<sup>†,§</sup> Wen Han Chong,<sup>‡</sup> Yuhua Feng,<sup>‡</sup> Xiaohui Song,<sup>‡</sup> Chu Long Tham,<sup>§</sup> Jun Wei,<sup>\*,§</sup> Ming Lin,<sup>\*,¶</sup> and Hongyu Chen<sup>\*,†,‡</sup>

<sup>†</sup>Institute of Advanced Synthesis, School of Chemistry and Molecular Engineering, Jiangsu National Synergetic Innovation Center for Advanced Materials, Nanjing Tech University, Nanjing 211816, China

<sup>‡</sup>Division of Chemistry and Biological Chemistry, School of Physical and Mathematical Sciences, Nanyang Technological University, Singapore 637371

<sup>§</sup>Singapore Institute of Manufacturing Technology, Agency for Science, Technology and Research, Singapore 637662

<sup>¶</sup>Institute of Materials Research and Engineering, Agency for Science, Technology and Research, Singapore 138634

### S Supporting Information

**ABSTRACT:** World's smallest screws with helical threads are synthesized via mild etching of Ag nanowires. With detailed characterization, we show that this nanostructure arises not from the transformation of the initial lattice, but the result of a unique etching mode. Three-dimensional printed models are used to illustrate the evolution of etch pits, from which a possible mechanism is postulated.

Chirality is common in our daily life as it is present in screws, gears, nuts, and bolts. For creating nanoscale chiral features, there are only few synthetic pathways available, and the level of morphological control is still far from adequate. Expanding synthetic methodology is thus a crucial step toward the “total synthesis” of nanoscale architectures. To date, nearly all chiral nanostructures were synthesized by growth or assembly, either in gas or solution phase.<sup>1</sup> The asymmetric growth phenomena and their underlying reasons are relatively well studied and reviewed.<sup>1c</sup> Being the opposite of growth, etching provides an equal synthetic window, but it has rarely been explored for creating chiral nanostructures.

Typically, the equivalent facets of nanostructures would etch equivalently and the symmetrical removal of substances always leads to achiral products. For instance, the {100} facets of Ag octahedra can be selectively etched with NH<sub>3</sub> and H<sub>2</sub>O<sub>2</sub> in the presence of poly(vinylpyrrolidone) (PVP), giving Ag octapods.<sup>2</sup> Tetraoctylammonium and Br<sup>-</sup> ions were used to passivate either {111} or {100} facets of Au microcrystals, creating nanoscale pits of regular shapes.<sup>3</sup> From these prior etching examples, capping ligands are of great importance in stabilizing specific facets,<sup>2,3</sup> so that well-defined geometric shapes could emerge. Mild etchants are often required to avoid rapid isotropic etching.<sup>2</sup>

In this work, nanoscrews are synthesized by mild etching of pentagonal Ag nanowires (Figure 1). We study the asymmetrical etching mode to understand the inequivalent etching of the equivalent facets. Etching begins at the twin boundaries creating faceted pits. Instead of symmetrical expansion forming circular threads around the nanowire, the etch pits prefer to merge at an angle and the demand for low surface energy causes the resulting ridges and grooves to spiral around the nanowire.

The as-synthesized pentagonal Ag nanowires (80–180 nm)<sup>4</sup> were purified repeatedly to remove the excess PVP, before being

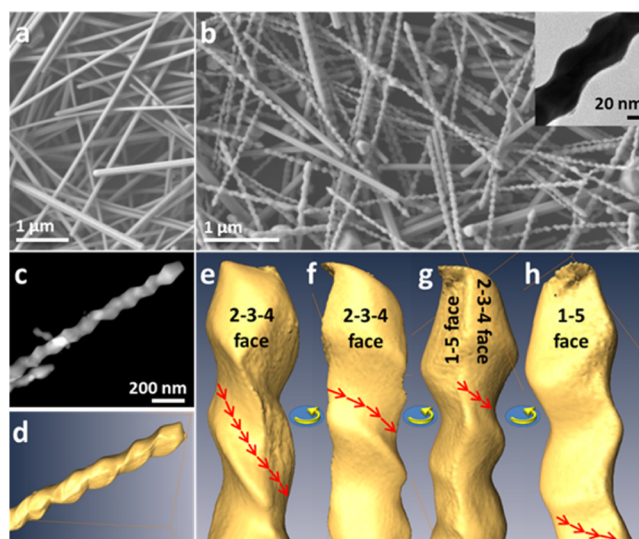


**Figure 1.** SEM images of (a) the as-synthesized Ag nanowires and (b) those after etching. Insets show the TEM images of a typical etched nanowire. (c) HAADF STEM image and (d) reconstructed tomography volume of a selected nanowire segment. (e–h) Screen shots showing the reconstructed volume at different perspectives.

attached to an NH<sub>2</sub>-functionalized Si wafer chip. The chip was then treated with AgNO<sub>3</sub> in ethylene glycol at 80 °C for 20 min. The remaining solution showed no observable volume change due to evaporation, and it was washed off with water. This mild etching step was repeated five times. The resulting sample can be directly characterized by scanning electron microscopy (SEM) or sonicated in a solution to transfer the nanowires for transmission electron microscopy (TEM) characterization. To our great interest, the etched nanowires showed obvious undulation (~87% yield, Figures 1b and S1a) indicating a possible chiral structure. In contrast, a single-step etching with prolonged reaction time (100 min) does not yield any similar structure (Figure S2f). It appears that the multiple etching-washing cycles are critical for the continual removal of PVP.

Received: June 17, 2016

Published: August 11, 2016

Scanning transmission electron microscopy (STEM) tomography was performed for better visualization. The reconstructed volume is presented in Figure 1d–h, with comparison to its high angular dark field (HAADF) STEM image (Figure 1c). Obviously, the equivalent facets/edges of the initial nanowires did not etch equivalently, otherwise the original 5-fold symmetry would have been retained, arriving at an achiral product. Detailed observation indicates that the etched nanowire has a pseudohelical morphology; there is a flat face causing the helical threads to be noncontinuous. Of the original facets, the 2–3–4 face develops helical features, whereas the 1–5 face becomes nearly flat. Nonetheless, the smooth ridges and grooves are reminiscent of screw threads and indicative of a concerted etching process.

The results clearly defy the initial pentagonal symmetry of the nanowire, unlike the typical etching reported in the literature. A simple explanation of facet-specific etching would be insufficient to account for the concerted etching with symmetry breaking. While it is unlikely that the Ag nanowires would have intrinsic chirality in its crystal structure, we still have to examine the possibility. First, we need to understand the structures of the initial and product nanowires, so that the inherited structure and the resulting differences can be clearly assigned.

Ag nanowires from polyol synthesis are known to have face-centered cubic (FCC) crystal structure and 5-fold twinning.<sup>5</sup> Diffraction patterns can only be obtained from specific zone axes (Figure S3),<sup>5a,c</sup> whereas the contribution from misaligned domains is always too weak to be seen. The selected area electron diffraction (SAED) pattern in Figure 2b shows two sets of diffraction, corresponding to the crystal domains orientated at the [211] and [100] zone axes (three of the five crystal domains appear in the diffraction).<sup>5c</sup> The same SAED patterns are

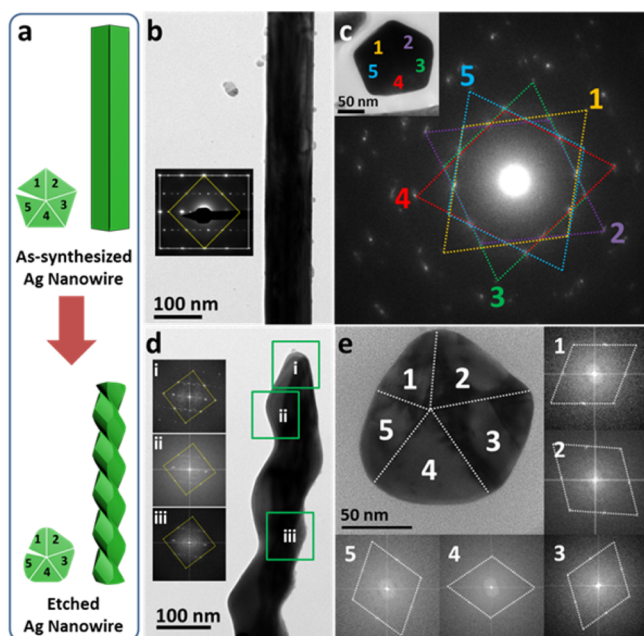


**Figure 2.** (a) Schematics illustrating the asymmetric etching. (b) TEM image and SAED pattern (inset) of a typical Ag nanowire. (c) SAED and TEM image (inset) of a Ag nanowire cross section, with numbers indicating the five crystal domains. (d) TEM image and regional FFTs (inset) of an etched nanowire, with similar orientation as the nanowire in (b). (e) TEM image of a cross section of an etched nanowire, with the corresponding FFTs of the five crystal domains.

observed in all of the etched Ag nanowires we have examined (Figure S7), ruling out the possibility that a few nanowires with unexpected chiral lattice may be responsible for the observed nanoscrews. In addition, the fast Fourier transform (FFT) images obtained from different regions of the nanowire showed the same orientation and patterns (Figure 2d inset), suggesting the absence of twisting. Hence, the crystal structure is inherited during the etching, ruling out any lattice transformation.

Cross sections of the Ag nanowires were prepared as thin slices (about 70 nm) using microtome.<sup>6</sup> The initial Ag nanowires gave star-shaped SAED patterns consisting of five overlaying diamonds along  $\langle 110 \rangle$  zone axes, as highlighted in Figure 2c.<sup>5a,g</sup> After etching, a similar SAED pattern (Figure S8) was observed, indicating an unchanged lattice. Shown in Figure 2e are the FFTs obtained at the five respective crystal domains; they are essentially the constituent diamond-shaped patterns. The initial nanowire showed a pentagonal cross section; after etching, it became more rounded as the twin defects at the edges promote etching. In particular, one of the twin boundaries was significantly more etched than the rest. For convenience of discussion, we labeled the five crystal domains so that the flattened boundary sits between Crystal 1 and 5, giving the 1–5 face.

“Cross sections” can also be extracted from the tomography data (Figure S9), which are thinner than the real ones obtained by microtome. Periodic changes were observed in the 2–3–4 face, whereas the 1–5 face showed only minor changes, consistent with the overall flat side (Figure 1h). It is known in the literature that five FCC crystals with  $\{111\}$  interface cannot fill space, leaving a “gap” of  $7.35^\circ$  (Figure 2a).<sup>5b,d,e</sup> This misfit is reflected in the slight misalignment of the  $\{111\}$  SAED spots (Figure 2c),<sup>5a</sup> and further analysis of the FFTs shows that the misfit is distributed among all five twinned boundaries (Figure S10).<sup>7</sup>

Given the size distribution of the nanowires, it is surprising that the nonetched nanowires were always the thicker ones ( $>100$  nm), whereas etching was always thorough for the thinner ones, i.e., no nanowire with half transformed helical segment was observed. As summarized in Figure S1, the etched nanowires became obviously thinner, but the thicker ones did not show noticeable changes in diameter. Such different etching modes were unlikely caused by the chemical environments, as these nanowires were anchored at the same location. It can be better explained by the concurrent ripening (*vide infra*).<sup>8</sup>

As a comparison, thick Ag nanowires of 300–500 nm diameter were synthesized,<sup>6</sup> and more etching cycles were applied. Figure 3a–c show that these thick nanowires can still be etched. As the etching was relatively slow, the results provide an opportunity to observe the intermediates: Instead of direct emergence of helical features, the nanowires showed pits of similar size with hexagonal outline. They typically started as a line of small pits along the twin boundaries, with some remaining  $\{100\}$  facets (Figure 3b). The small difference in their size suggests a certain degree of randomness in the time and location of their formation. As they enlarged in dimension, the pits merged together with those from the adjacent twin boundaries (Figure 3c), eliminating the initial  $\{100\}$  facets and forming primary grooves, but the regular-shaped outlines can still be recognized, suggesting that the surface in the pits is still faceted.

In the literature, etch pits formed in the  $\{100\}$  facets of bulk, single-crystalline Ag usually give inverse square pyramids with  $\{111\}$  internal facets.<sup>9</sup> If such a pit occurs at a twin boundary, we would expect a rectangular pit, rather than the hexagonal ones.



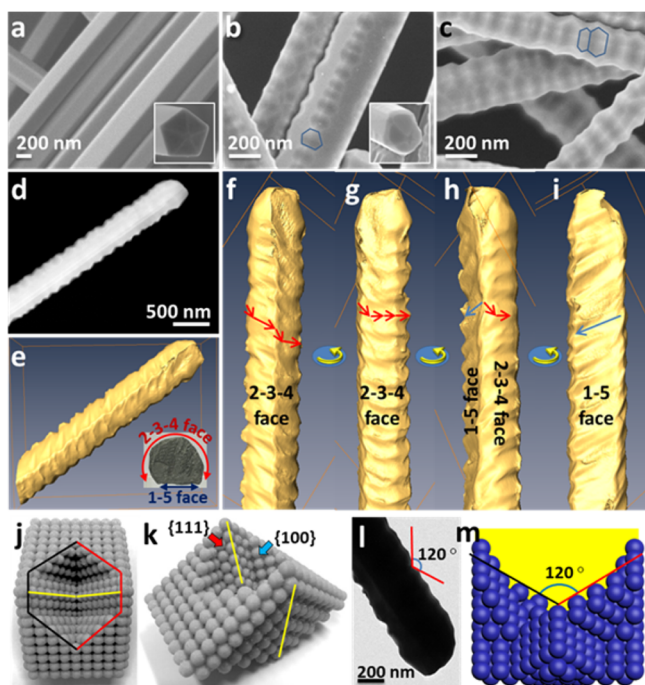


**Figure 3.** SEM images of (a) as-synthesized Ag nanowires with 300–500 nm diameter; (b) slightly etched Ag nanowires with remaining [100] facets; and (c) Ag nanowires with all of their [100] facets etched away forming grooved structures. (d) HAADF STEM image and (e) reconstructed tomography volume of a thick nanowire after etching, with a “cross section” shown in the inset. (f–i) Screen shots showing the reconstructed volume at different perspectives. (j,k) Three-dimensional printed model showing the etch pit and the exposed facets at different perspectives. The twin boundary is highlighted in yellow. (l) TEM image of a Ag nanowire showing the side view of the etch pits; the pits on the opposite side are misaligned based on SAED analysis. (m) Three-dimensional model of an etch pit orientated at the [111] zone axis, the same orientation as in (l).

PVP is known to passivate Ag {100} and {111} facets,<sup>10</sup> which are the enclosing facets of the initial Ag nanowires. Considering the large molecular weight of PVP in our system (MW = 55000), we speculate that its multiple binding groups would allow it to persist on the Ag surface. This argument is supported by (1) the faceted etch pits; (2) the necessity of multiple etching-washing cycles; and (3) the gradual loss of facets (becoming smooth and rounded) with more cycles. After extensive trials, we found that an etch pit with {111} and {100} internal facets would give a hexagonal outline, as shown in the 3D printed model (Figure 3j,k).

One of the thick nanowires with more extensive etching was selected for STEM tomography (Figure 3e–i). As observed from the reconstructed volume, the initial {100} facets were now beyond recognition. The 1–5 face was almost etched flat (Figure 3i), more extensive than the 2–3–4 face. This difference is further confirmed by the “cross section” of the 3D printed model (Figure 3e inset) and the tip of a nanowire in SEM (Figure 3b inset). In contrast to the aligned hexagons and perpendicular “grooves” in Figure 3b,c, the reconstructed volume shows tilted ridges and grooves: Those on the 1–5 face are somewhat slanted (blue arrows), whereas those on the 2–3–4 face are spirals not exactly perpendicular to the length of the nanowire (red arrows). It appears that the ridges and grooves tilt progressively with the extent of etching: no tilting in Figure 3b; a few slanted lines in

Figure 3c; most of the ridges/grooves are tilted in Figure 3f–i; and the prominent undulations for the thinner ones in Figure 1.

For convenience of visualization, we 3D printed the reconstructed tomography volume (see videos in the SI). The surfaces of both thin and thick nanowires (Figures 1 and 3) are rather smooth, consistent with the gradual loss of PVP after repeated etching-washing cycles. As a result, however, we could no longer assign the exposed facets.

As the pits are deepest at the twin boundaries, we oriented the nanowires so that one of the twin planes became perpendicular to the electron beam, hoping to view the intersecting facets from the side. However, only notches with around 120° opening angle were observed. Such an angle does not fit the dihedral angle of any low-index facets.<sup>11</sup> It was until the 3D model of the proposed pit was printed that we realize the difficulty in direct viewing the intersecting facets from the side (Figure 3j,k). In fact, the 120° angle is defined by the projection of the ridges as illustrated by the red and black lines in Figure 3j,m, only when the twin plane is positioned parallel to the plane of the paper. Without proper orientation, the intersecting ridges and facets will show varying angles depending on the perspective.

One may argue that the thin and thick nanowires etched differently due to the specific etching conditions. To investigate this possibility, we premixed the thick and thin nanowires before attaching them onto a silicon wafer. With the exact same etching environment, unchanged results were still obtained, i.e., etch pits appeared on the thick nanowires, whereas the thin ones gave extensively etched helical structures (Figure S12). We speculate that concurrent ripening is responsible, as its contribution would accumulate with the multiple cycles of extremely slow etching. Typically, ripening would cause thick nanowires to grow and thin ones to dissolve. Adding this ripening process to the overall etching would accelerate the etching of thin nanowires and cause the thick ones to etch slower, hence leading to the different extent. Therefore, the thick and thin nanowires in a sample would etch differently, whereas the different segments of any individual nanowire would etch uniformly. Control experiments showed that Ag<sup>+</sup> ions were critical for the transformation (Figure S15), supporting the ripening argument.

Formation of chiral structures from achiral nanowires requires a key step of symmetry breaking. Simply enlarging the pits with equivalent facets would be insufficient. As illustrated in Figure 4g,

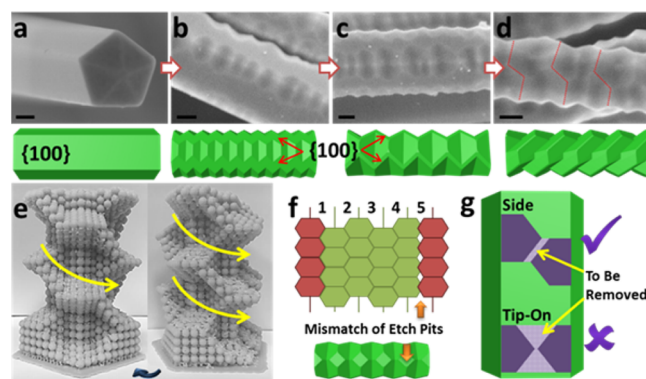


**Figure 4.** Schematics illustrating (a–d) the progress of etch pits leading to the pseudo helical structure; (e) 3D printed model showing the proposed grooves after etching and (f) mismatch of the etch pits with the 5-fold symmetry; (g) the hexagonal pits prefer merging at an angle, as the tip-on merging requires more materials to be removed and is thus less likely. Scale bars are 100 nm.

merging the pits tip-on would require a lot of materials to be removed. In contrast, merging the pits from the side would only require a thin “wall” to be removed leading to a slanted groove and breaking the symmetry. Considering the slow etching with concurrent ripening, we postulate that the system seeks lower surface energy by making smooth ridges and grooves. Hence, once a thin “wall” is broken (Figure 4c–e), the subsequent etching would always cause the same groove to get more entrenched, rather than diverting toward a new direction. Forming a spiral with smooth ridges and grooves would be preferred and further etching would only expand and deepen the grooves. On the other hand, “wrong” direction of wall breaking may accidentally occur at a few places. The resulting sharp turns and corners would be preferentially etched. It is conceivable that many steps of merging are required from the primary pits and grooves (Figure 4b,c) to the deep and wide grooves of the eventual helical structure (Figures 4d and 1).

Figure 4f shows the 2D layout of the hexagonal pits around the nanowire. It is clear that they cannot fit nicely together due to the odd number of faces. As a result, many sharp edges and corners are expected at such a misfit boundary (Figure 4f), which would be preferentially removed during the etching. Hence, there are at least two possible ways to explain the extensive etching at the flattened 1–5 face (Figures 1h and 2e): (1) maybe the  $7.35^\circ$  misfit angle is distributed more at one of the twins;<sup>5d,e</sup> or (2) the new argument on the mismatch of etch pits with the 5-fold symmetry. While the evidence are against 1 (Figure S10),<sup>7</sup> it is still possible that both factors may coincide and promote etching.

In summary, we demonstrate that it is indeed possible to achieve delicate control in etching, converting pentagonal Ag nanowires into nanoscrews with helical threads. In the unique etching mode, symmetry breaking occurs at the slanted merging of hexagonal etch pits, and the combined etching and ripening processes are critical for entrenching the smooth grooves and guiding the complex etching toward coherent helical features.

It is interesting to note that a 3D-printed model is far more effective than a computer model in terms of visualization. The eye-hand coordination and visual interpretation are difficult to achieve *in silico*, particularly for an untrained person and with limited computer processing power.

## ■ ASSOCIATED CONTENT

### ● Supporting Information

The Supporting Information is available free of charge on the ACS Publications website at DOI: 10.1021/jacs.6b06250.

Characterization and synthesis methods, and Figures S1–S17 (PDF)

Thin nanowire tomography (MPG)

Thick nanowire tomography (MPG)

Thin nanowire (MPG)

Thick nanowire (MPG)

## ■ AUTHOR INFORMATION

### Corresponding Authors

\*hongyuchen@ntu.edu.sg

\*m-lin@imre.a-star.edu.sg

\*jwei@simtech.a-star.edu.sg

### Notes

The authors declare no competing financial interest.

## ■ ACKNOWLEDGMENTS

The research was supported by A\*STAR (SERC 112-120-2011) and MOE (RG14/13) of Singapore. The authors would like to thank Dr. Chong Huang Ming for his assistance in 3D printing of the structures.

## ■ REFERENCES

- (1) (a) Gao, P.-X.; Liu, G. In *Three-Dimensional Nanoarchitectures: Designing Next-Generation Devices*; Zhou, W., Wang, L. Z., Eds.; Springer: New York, 2011; pp 167–204. (b) Meng, F.; Morin, S. A.; Forticaux, A.; Jin, S. *Acc. Chem. Res.* **2013**, *46*, 1616–1626. (c) Wang, Y.; Xu, J.; Wang, Y.; Chen, H. *Chem. Soc. Rev.* **2013**, *42*, 2930–2962. (d) Ren, Z.; Gao, P.-X. *Nanoscale* **2014**, *6*, 9366–9400. (e) Zhu, Y.; He, J.; Shang, C.; Miao, X.; Huang, J.; Liu, Z.; Chen, H.; Han, Y. *J. Am. Chem. Soc.* **2014**, *136*, 12746–12752.
- (2) Mulvihill, M. J.; Ling, X. Y.; Henzie, J.; Yang, P. *J. Am. Chem. Soc.* **2010**, *132*, 268–274.
- (3) Mettela, G.; Kulkarni, G. *Nano Res.* **2015**, *8*, 2925–2934.
- (4) Korte, K. E.; Skrabalak, S. E.; Xia, Y. *J. Mater. Chem.* **2008**, *18*, 437–441.
- (5) (a) Elechiguerra, J. L.; Reyes-Gasga, J.; Yacaman, M. J. *J. Mater. Chem.* **2006**, *16*, 3906–3919. (b) Mayoral, A.; Barron, H.; Estrada-Salas, R.; Vazquez-Duran, A.; Jose-Yacaman, M. *Nanoscale* **2010**, *2*, 335–342. (c) Sun, Y. *Nanoscale* **2010**, *2*, 1626–1642. (d) Sun, Y.; Ren, Y.; Liu, Y.; Wen, J.; Okasinski, J. S.; Miller, D. J. *Nat. Commun.* **2012**, *3*, 971. (e) Zhu, L.; Shen, X.; Zeng, Z.; Wang, H.; Zhang, H.; Chen, H. *ACS Nano* **2012**, *6*, 6033–6039. (f) Sun, Y. *Chem. Soc. Rev.* **2013**, *42*, 2497–2511. (g) McCarthy, E. K.; Bellew, A. T.; Sader, J. E.; Boland, J. J. *Nat. Commun.* **2014**, *5*, 5336.
- (6) Supporting Information.
- (7) (a) Zhang, S.-H.; Jiang, Z.-Y.; Xie, Z.-X.; Xu, X.; Huang, R.-B.; Zheng, L.-S. *J. Phys. Chem. B* **2005**, *109*, 9416–9421. (b) Zhou, Y.; Fichthorn, K. A. *J. Phys. Chem. C* **2014**, *118*, 18746–18755.
- (8) Voorhees, P. W. *J. Stat. Phys.* **1985**, *38*, 231–252.
- (9) Kawabuchi, K. *J. Cryst. Growth* **1971**, *11*, 92–94.
- (10) (a) Al-Saidi, W. A.; Feng, H.; Fichthorn, K. A. *Nano Lett.* **2012**, *12*, 997–1001. (b) Saidi, W. A.; Feng, H.; Fichthorn, K. A. *J. Phys. Chem. C* **2013**, *117*, 1163–1171. (c) Zhou, Y.; Saidi, W. A.; Fichthorn, K. A. *J. Phys. Chem. C* **2013**, *117*, 11444–11448.
- (11) Brigham Young University. Crystal Planes in Semiconductors. [http://www.cleanroom.byu.edu/EW\\_orientation.phtml](http://www.cleanroom.byu.edu/EW_orientation.phtml) (accessed May 19, 2016).